Design and Analysis of Localized DNA Hybridization Chain Reactions

*Hieu Bui, Vincent Miao, Sudhanshu Garg, Reem Mokhtar, Tianqi Song, and John Reif**

Theoretical models of localized DNA hybridization reactions on nanoscale substrates indicate potential benefits over conventional DNA hybridization reactions. Recently, a few approaches have been proposed to speed-up DNA hybridization reactions; however, experimental confirmation and quantification of the acceleration factor have been lacking. Here, a system to investigate localized DNA hybridization reactions on a nanoscale substrate is presented. The system consists of six metastable DNA hairpins that are tethered to a long DNA track. The localized DNA hybridization reaction of the proposed system is triggered by a DNA strand which initiates the subsequent self-assembly. Fluorescence kinetics indicates that the half-time completion of a localized DNA hybridization chain reaction is six times faster than the same reaction in the absence of the substrate. The proposed system provides one of the first known quantification of the speed-up of DNA hybridization reactions due to the locality effect.

1. Introduction

DNA hybridization reactions based on toehold-mediated strand displacement have been studied in the past decade and widely used to operate nanoscale machines and construct DNA circuits.[1–13] The kinetics of DNA hybridization reactions depends on diffusion of DNA molecules which randomly collide and interact in a 3D fluidic space. To speed-up DNA hybridization reactions, a high concentration of DNA molecules is often employed; however, leaks and crosstalk frequently occur in the reactions at high concentrations. As a result, unintended DNA hybridization reactions impede the desired DNA hybridization reactions from happening. Recently, theoretical models to describe DNA hybridization reactions on nanoscale substrates have been proposed.[14–17] The models indicate strong evidence of speed-up as well as leak reduction when DNA gates are tethered to the substrates. In terms of experimental demonstration, Kopperger et al. studied the diffusive transport mechanism of linear DNA strands bound to the surface of DNA origami rectangle using surface-bound sticky strands.[18] Teichmann et al. expanded the work of Kopperger et al. by exploring the effect of spatial arrangement of DNA strands on the surface of DNA origami.[19] From understanding the spatial arrangement of DNA molecules on nanoscale surfaces, Ruiz et al. created a simple see-saw DNA amplifier circuit that could operate on the surface of DNA origami.[20] Prior studies often tethered DNA strands to the surface of DNA nanostructures to exploit the locality effect. However, the strands are free to diffuse beyond the reaction volume during hybridization. When the DNA strands are not physically attached to the surface, the likelihood of having DNA strands flow away from the surface during hybridization is higher than when the strands are physically tied down to the surface. Recently Yin et al. employed triggered self-assembly hybridization chain reaction (HCR)[21–25] to program DNA that could form and grow nanoscale structures ranging from

H. Bui, Dr. S. Garg, R. Mokhtar, T. Song, Prof. J. Reif
Department of Computer Science
Duke University
308 Research Drive, Campus Box, 90129, 27708, USA
E-mail: reif@cs.duke.edu
V. Miao
Department of Biomedical Engineering
Duke University
101 Science Drive, Campus Box, 90281, 27708, USA

DOI: 10.1002/smll.201602983

ADVANCED SCIENCE NEWS
www.advancedsciencenews.com

small oligomers to branched oligomers and even dendritic oligomers.[26,27] Inspired by the triggered self-assembly HCR and the potential speed-up from tethering DNA reactions to the surface, we present a system to study DNA hybridization chain reactions on a nanoscale surface. In particular, the proposed system consists of six metastable DNA hairpins that are bound to a long 90-nucleotide DNA strand. The use of metastable DNA hairpin provides the following advantages over the regular DNA strand: (i) it acts as an anchor to fasten the entire structure to substrates such as DNA nanostructures via DNA hybridization or other surfaces via chemistry linkers like biotin–streptavidin, (ii) it acts as a carrier to transport cargo from one position to the other, and (iii) it acts as a flexible linker to connect the carrier to the anchor, thus preventing the cargo from flowing away during hybridization. Experimental results provide strong evidence that the speed-up of DNA hybridization reactions is due to the locality effect.

1.1. Sequence Design

A specific design of localized DNA hybridization chain reactions consists of a long DNA strand (LT), a set of six metastable DNA hairpins (H_1, H_2, H_3, H_4, H_5, H_6), and an initiator (I) as shown in **Figure 1**A. The long DNA strand, also called the DNA track, provides complementary binding domains to assemble the six hairpins together. Each DNA hairpin consists of a stem, a loop, and a sticky end. The stem consists of two domains (C_i and R) to form a stable duplex with 14 base pairs. The loop consists of two clamp domains (C_{i-1} and C_{i+1}), a linker domain (L), and a sequestered domain (S_{i+1}). The two clamp domains within the loop are programmed i) to ensure the incoming hairpin from going back to the previous state (i.e. C_{i-1}) and ii) to provide a place to fasten the next hairpin (i.e. C_{i+1}) upon hybridization. The linker domain is served as a flexible rope and can be tuned to accommodate for different spatial arrangements among hairpins. Prior systems[21,24] had to be tailored to have a stem of 18 base pairs and a toehold/hairpin loop region of 6 nt. The clamp domains enable us to design systems with variable stem and toehold lengths, thus it increases the sequence space and applicability. The sticky end consists of an external toehold domain (S_i) that is complementary to the loop domain (S_{i+1}) of hairpin (H_{i+1}), a spacer domain (T_i) to offset potential geometrical constraints, and an anchor domain (A_i) to attach the hairpin (H_i) to the long DNA track. Hairpins are distinguishable by two single-stranded toehold domains (S_i and S_{i+1}) – one toehold is external (a single-stranded sticky end, readily available for hybridization) and one is sequestered within the hairpin loop. The stem (R) and linker (L) domains of all hairpins comprise of the same sequences. The spacer domain (T) is used to accommodate for potential geometrical constraints. The clamp domain (C) is implemented to minimize

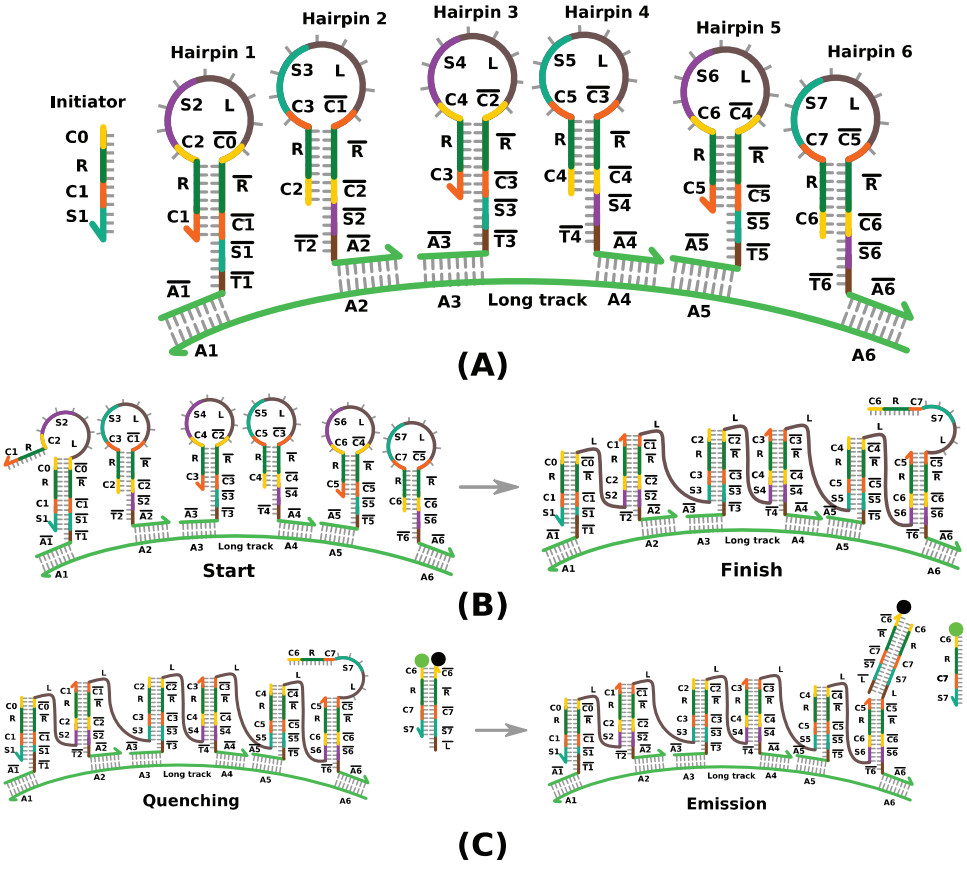

Figure 1. A) Components of localized DNA hybridization chain reaction system: six metastable DNA hairpins anchored to a long DNA track. Prior to the addition of the initiator, DNA hairpins do not hybridize. B) Triggered self-assembly of localized DNA hybridization chain reaction mechanism for the first and last steps. C) Fluorescence reporting mechanism to observe the kinetics of localized DNA hybridization reaction.

the breathing effect at the ends of the DNA duplex and to ensure that the reaction proceeds forward.[28]

1.2. Mechanism of Localized DNA Hybridization Reaction

The mechanism of triggering localized DNA hybridization reactions is based on the assumption that all metastable DNA hairpins are successfully attached to the long DNA track. In addition, DNA hairpins are programmed to undergo cascade chain reactions such that the first hairpin only hybridizes to the adjacent hairpin and this process continues until the last hairpin is hybridized. Initially, all hairpin components are anchored to the long track but do not hybridize. The localized DNA hybridization chain reaction occurs when the initiator (I) is introduced. The initiator hybridizes to the external toehold (S_1) of H_1 and displaces the stem of H_1 by branch migration, opening the loop, and revealing its sequestered toehold domain (S_2) as illustrated in Figure 1B (left). The opened loop of H_1 can now hybridize to the external toehold of H_2 and displace the stem of H_2 by branch migration, opening the loop of H_2. A similar mechanism occurs until the stem of H_6 is displaced by the opened loop of H_5 as shown in Figure 1B (right). The entire localized cascade DNA hybridization chain reaction occurs on the long DNA track, thus the hairpins are readily available once triggered by the initiator and the kinetic rate is expected to happen faster than in the absence of the long DNA track. The use of hairpins enables active components to be physically attached to the surface during hybridization and the likelihood of losing active components is significantly lower than using regular strands from prior studies.[18–20]

2. Results and Discussion

The thermal equilibrium conditions of the proposed system were first studied by gel electrophoresis. In particular, DNA hairpin sequences were synthesized without the anchor domains. The self-assembly of those hairpins was analyzed using 10% native polyacrylamide gel electrophoresis (PAGE) as illustrated in **Figure 2** (left panel). Lane 1 contains a DNA marker with 20 bp increments. Lanes 2–7 contain a mixture of 1–6 hairpin(s) in the absence of the initiator. Products of low molecular weight are visible around 20–40 bp, indicating that individual hairpins remain intact although there is a slight evidence of crosstalk (undesired reactions in the absence of the initiator) in lanes 4–7 around 100–300 bp. Lanes 8–13 contain a mixture of 1–6 hairpin(s) in the presence of the initiator. Products of increasing higher molecular weight are visible and are indicated as marker maroon boxes. In addition, individual hairpin strands were mostly consumed by the cascade reactions. These controls indicate that the oligomers are forming due to the addition of the initiator with the expected lengths of ≈40, 80, 120, 160, 200, and 240 bp. The presence of residual hairpins of around 20–40 bp in lanes 8–13 could be due to stoichiometric concentration differences between DNA strands, improper synthesized DNA strands that did not participate in the reaction, or excess initiator strand. The successively higher molecular weight products from these controls indicate that DNA hairpins were programmed correctly and that the cascade hybridization reaction mechanism was well designed.

To observe the thermal equilibrium conditions of DNA hairpins bound to the long DNA track, DNA hairpin strands were synthesized with the anchor domains. Due to the

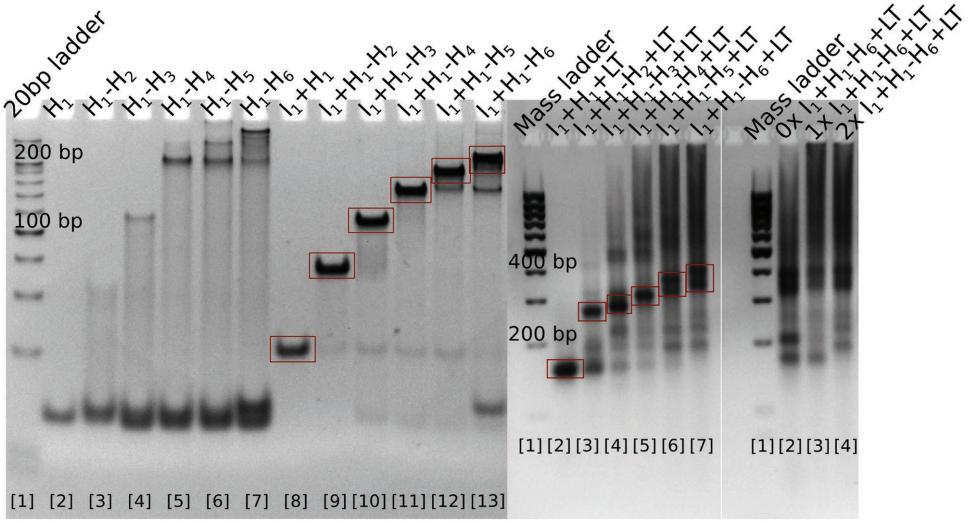

Figure 2. Left panel: 10% native PAGE gel analysis of HCR: All samples were incubated at room temperature for 200 min. All samples were prepared at 500×10^{-9} M and 34 µL of sample was loaded into each lane. All hairpins do not carry the anchor domains. Lane 1 contains DNA marker with 20 bp increments (20–300 bp). Lanes 2–7 contain mixture of different numbers of hairpins in the absence of the initiator. Lanes 8–13 contain the same corresponding mixture of hairpins in the presence of the initiator. Middle and right panels: 3% agarose gel analysis of localized DNA hybridization chain reaction (LCR). All hairpins are conjugated with the anchor domains to self-assemble to the long DNA track. All samples were quickly annealed for 10 min and incubated with the initiator for 200 min at room temperature. All samples were prepared at 500×10^{-9} M and 10 µL of sample was loaded into each lane. Middle panel: Step-by-step LCR—500×10^{-9} M of hairpins were mixed with 2× LT in the presence of 2× initiators (I). Right panel: Effect of initiator concentration to LCR—500×10^{-9} M of hairpins were mixed with 2× LT in the presence of the initiator. Note that the marker maroon boxes indicate major bands of the desired DNA structures.

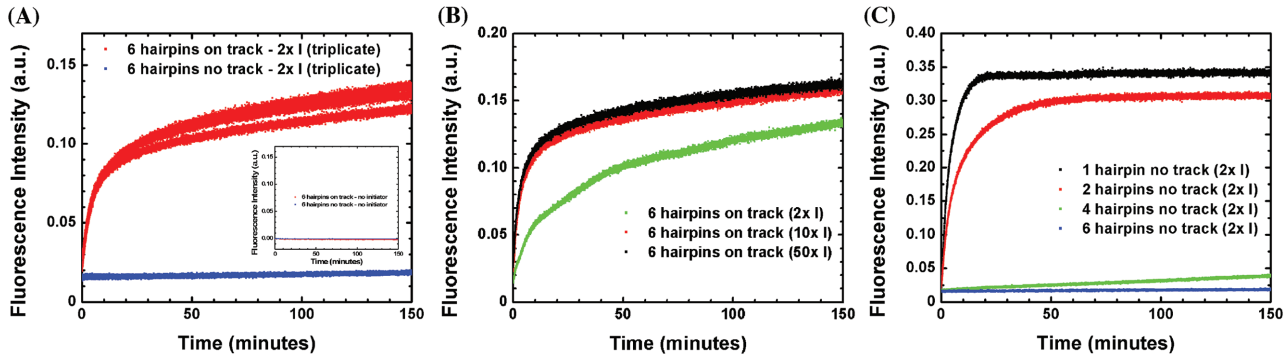

Figure 3. Kinetic characterization of triggered self-assembly hybridization chain reactions. A) Localized DNA hybridization chain reactions with and without the presence of the long DNA track in two times excess initiators. Note: inset shows the fluorescence responses of the same systems but in the absence of the initiator. B) Effect of localized DNA hybridization chain reaction rate as a function of initiator concentration. C) Control kinetic analysis of reactions as a function of hairpins in the absence of long DNA track.

addition of the long DNA track, the size of DNA hairpins bound to the track was larger than the porous size of 10% PAGE gel (data not shown). Thus the self-assembly of DNA hairpins on the track was analyzed using 3% agarose gel electrophoresis as shown in Figure 2 (middle panel). Lane 1 contains a DNA marker with 100 bp increments. Lanes 2–7 contain a mixture of 1–6 hairpins self-assembled on the track prior to the addition of the initiator. Individual hairpins hybridized and bound to the long DNA track as indicated with marker maroon boxes. The successively higher molecular weight products from these lanes indicate that the reactions occurred and resulted in higher products around 200–400 bp. Presence of residual bands below the marker boxes in lanes 2–7 could be due to stoichiometric concentration differences between DNA strands, or improper synthesized DNA strands. There is a broad distribution of product size above 400 bp in lanes 4–7, indicating a gradual increase in the population of multimers. These multimers could be further minimized by carefully adjusting the stoichiometry between DNA sequences or tuning the annealing temperature.

3% agarose gel was again used to study the effect of initiator concentration on the localized DNA hybridization reaction of DNA hairpins bound to the track as shown in Figure 2 (right panel). Lane 1 contains a DNA marker with 100 bp increments. Lane 2 contains a mixture of six hairpins self-assembled on the track in the absence of the initiator: the designed assembly is clearly visible at around 300–400 bp; however, there are still hairpin remains below 200 bp marker. Lanes 3 and 4 contain a mixture of six hairpins self-assembled on the track in the presence of 1× and 2× initiator concentrations, respectively. The designed assemblies are visible in both lanes and at the same location around 300–400 bp. Inferring from the intensities in all lanes, the broad distribution of multimers above 400 bp marker appears stronger in the presence of the initiator (lanes 3 and 4) than in the absence of the initiator (lane 2), indicating localized reactions occurred due to the presence of the track.

To observe the kinetics of localized DNA hybridization chain reaction (LCR) of DNA hairpins bound to the long DNA track, a fluorescence-based method was implemented. In particular, an independent reporter complex was designed with a pair of fluorophore and quencher molecules (Figure 1C). The reporter complex was programmed to only bind to the LCR system after the cascade reaction was completed. **Figure 3**A shows the fluorescence kinetic response of six metastable DNA hairpins triggered by two times excess initiators. These hairpin strands were synthesized with the anchor domains. The blue curves are fluorescence responses of six DNA hairpins in the absence of the long DNA track. The red curves are fluorescence responses of six DNA hairpins in the presence of the track. The fluorescence data indicate that the localized DNA hybridization reaction occurred rapidly compared to the nonlocalized DNA hybridization reaction. Without the presence of the initiator, the minimal fluorescence signal was observed in both systems (inset, Figure 3A).

To study the effect of initiator concentration on the cascade-localized DNA hybridization reactions, various initiator concentrations were added to the same sample consisting of six DNA hairpins bound to the long DNA track as shown in Figure 3B. The fluorescence results indicate that insignificant changes are achieved in the presence of more than 10 times excess initiator. The saturation of the rate at 10–50 × initiator might also indicate that the interaction between the last hairpin and the quencher-labeled DNA strand is becoming rate limiting. This means that the localized reaction could be accelerated if the fluorescence reporting mechanism was a part of the last hairpin. In fact, we attempted to test a similar system in which the last hairpin was labeled with a fluorescence purine base (2-aminopurine) in order to overcome the rate-limiting factor from using the independent reporter complex. The fluorescence emission result was significantly less pronounced for the system with the concentration below 1×10^{-6} M (data not shown). As mentioned earlier, one of the benefits of exploring localized DNA hybridization reactions is to speed-up the reaction at low concentration to avoid leaks (unintended reactions in the absence of the input strand). Other approaches such as (i) labeling the last hairpin with the reporter complex which could potentially alter the kinetics of the hairpin structure or (ii) using excessive amount of the independent reporter complex to bias the bimolecular process to the pseudo-unimolecular process, could be explored.

To observe the effect of the anchor domains on the overall cascade reaction rate, different samples of DNA

hairpins were synthesized in the absence of the long DNA track as shown in Figure 3C. Upon adding the initiator, the fluorescence emission increases rapidly up to 20 min for the sample with a single hairpin (black curve) and 40 min for the sample with a pair of hairpins (red curve). Both samples slowly increase as thermal equilibrium was achieved. However, the fluorescence emission occurs slowly for the sample with four hairpins (green curve) and for the sample with six hairpins (blue curve). These results indicate that the reaction rates are slow and never reach thermal equilibrium within the experimental time scale (≈1000 min). As indicated by the leftmost gel data in Figure 2, the cascade reaction reached thermal equilibrium within 200 min for DNA hairpins which were synthesized without the anchor domains. Thus the addition of the anchor domain is possibly the reason that such minimal fluorescence was observed for systems with more than four hairpins in the absence of the long DNA track (blue curves, Figure 3A). To further demonstrate the effect of the anchor domain, the identical DNA hairpin system (blue curve, Figure 3C) was synthesized without the anchor domain. Multiple fluorescence experiments indicate that the designed cascade reaction occurred as expected and that the fluorescence emission was pronounced within the experimental time scale as illustrated in **Figure 4**A. An addition of an anchor domain to assist each DNA hairpin hybridizing to the long DNA track clearly affects the reaction kinetics.

To establish a systematic approach to measure the speed-up from tethering DNA hairpins on the long DNA track, multiple fluorescence experiments were performed for two samples—one sample was synthesized with six DNA hairpins bound the long DNA track, the other sample was synthesized with six DNA hairpins without the anchor domains. All fluorescence experiments were normalized to unity which is corresponding to thermal equilibrium. Figure 4A,B show reproducible fluorescence experimental results for the two samples. In particular, fluorescence results for six DNA hairpins (no anchor domain, no track) in the presence of 2× excess initiators are shown in Figure 4A. And, fluorescence results for six DNA hairpins bound to the long DNA track in the presence of 2× excess initiators are shown in Figure 4B. Note that the fluorescence experimental data in Figure 4B are the same results as Figure 3B but in replicate.

To quantify the speed-up resulting from tethering DNA hairpins to the long DNA track, we first describe the designated reaction pathways for the cascade DNA hybridization chain reactions of six hairpin gates in the presence and absence of the long track (illustrated in Figure 4C). In both cases, the initiation and the reporting mechanisms depend on the diffusion rates (k_i and k_o) of the initiator to the first hairpin gate and of the last hairpin to the reporter complex; these two processes are better described as bimolecular reactions (dashed boxes). In the absence of the track, the cascade hybridization chain reaction of six hairpins is treated as a bimolecular reaction, and because all the hairpins have a similar structure, they are assumed to have the same rate constant (k_s). In the case of six hairpin gates bound to the track, the

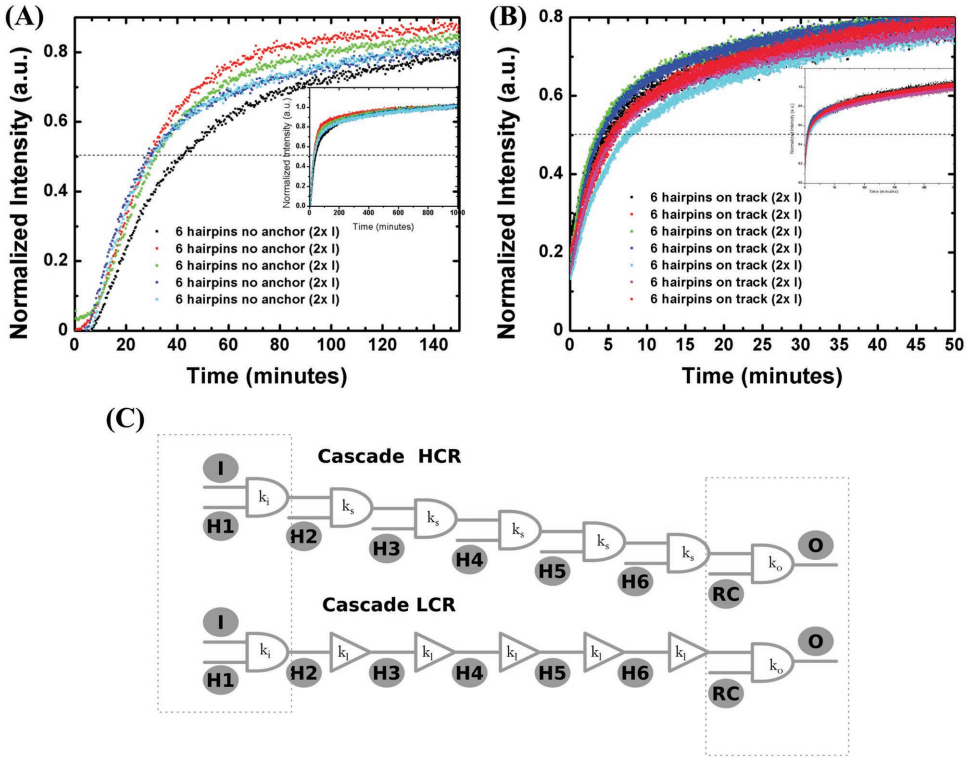

Figure 4. Reproducible fluorescence experimental results of the two systems which are then used to quantify the speed-up from tethering DNA hairpins on the long DNA track: A) six DNA hairpins (no anchor domain, no track) in the presence of 2× initiators, B) six DNA hairpins bound to the long DNA track in the presence of 2× initiators. Note: Dashed lines indicate half-time completion—the time required for the reaction to reach 50% completion. C) Model to describe cascade reactions with and without the locality effect. Note: AND symbol indicates bimolecular reaction; TRIANGLE symbol indicates unimolecular reaction.

localized cascade hybridization chain reaction is treated as a unimolecular reaction and all the hairpins are assumed to interact with the same rate constant (k_1). It is worth noting that the rate constant for the bimolecular reaction depends on the concentration of individual hairpins. In contrast, the rate constant for the unimolecular reaction is independent of the concentration of individual hairpins assuming all hairpins are assembled correctly on the track substrate. For our systems, the ensemble rate constant is a superposition of either multiple bimolecular processes (cascade HCR) or multiple unimolecular and bimolecular processes (cascade LCR). A reasonable quantity that can be used to measure the speed-up factor is the half-time completion for both systems as illustrated by dashed lines in Figure 4A,B. The half-time completion of the cascade DNA hybridization chain reactions of six hairpins was determined to be 32.77 min, indicating that half of hairpin population was consumed in the reaction. The half-time completion of the localized DNA hybridization chain reactions of six hairpins was determined to be 5.31 min. Independent of the multiple rate constants that dictated our systems, the empirical data indicate that the localized reaction experiences a factor of six times speed-up compared to the nonlocalized reaction.

To estimate the ensemble rate constants for our systems, we further assumed both systems experience the same kinetic effect arising from initiation and termination. Hence, the ensemble rate constant is inversely proportional to the half-time completion of the reaction. For the bimolecular reaction, the reaction rate depends on the initial concentrations of hairpins. For the unimolecular reaction, the reaction rate is independent of the initial concentrations of hairpins given that all hairpins correctly self-assembled on the track. The ensemble rate constant for cascade HCR was determined to be 1.017×10^5 M^{-1} s^{-1}. The ensemble rate constant for cascade LCR was determined to be 2.2×10^{-3} s^{-1}. Because the likelihood of having all hairpins attached to the long DNA track critically depends on the exact stoichiometry mixing, the assembly yield of the cascade LCR is expected to be harder to control than that of the cascade HCR. Although DNA hairpins bound to the long DNA track show evidence of cascade LCR, the distances between those hairpins have yet to be explored. Thermal equilibrium gel data and real-time fluorescence kinetic results indicate that the localized DNA hybridization reaction was clearly enhanced via tethering DNA hairpins to the long DNA track. For unlimited HCR with the assembly of multiple hairpin monomers, a larger surface area such as DNA origami could be employed. In particular, DNA origami rectangle designed by Rothemund[29] could accommodate up to 200 distinct addressable sites. In addition, the proposed system can be extended to form cyclic reactions by modifying the last hairpin to interact with the first hairpin which allows for the creation of longer oligomers.

3. Conclusion

With the goal of increasing the reaction rates, we experimentally demonstrated a surface-bound method by tethering hairpins to a long DNA track. The anchor domains which link the hairpins to the long DNA track have been shown to affect the reaction kinetics via fluorescence kinetic studies. The rate-limiting factor could be due to the independent reporter complex. We demonstrated an overall six times speed-up of localized DNA reactions over nonlocalized DNA reactions. It is important to note that this is an overall speed-up and not purely due to the localized hybridization reaction. The actual localized rate constant between a pair of hairpins still remains a challenge. Thus a new model for determining the localized rate constant is needed to fully measure the actual speed-up of the localized hybridization reactions. The proposed system provides one of the first known quantification of the speed-up of DNA hybridization reactions due to the locality effect. One possible approach to measure the localized rate constant is to tether the initiator to the surface and to label the last hairpin with the reporter complex. Ideally the initiation could be triggered by irradiation and the termination could be measured by the fluorescence emission from the last hairpin. This approach could possibly overcome the rate-limiting factor due to the initiation and the termination. In addition, we are currently investigating the localized hybridization chain reaction on the surface of DNA origami with a larger number of DNA hairpins. We conjecture that if we extend our experiments to have more than six hairpins on DNA origami, we will experience a much larger speed-up over nonlocalized hybridization reactions. We envision and are currently exploring the construction of Boolean logic, such as AND and OR gates, on the surface of DNA nanostructures. Recent advances in vitro evolution enabled the capability to generate a set of DNA aptamers that have a strong binding affinity to surface-bound proteins. Our proposed localized DNA hybridization reaction may be of practical use in performing surface computation on cellular membranes for disease detection and prevention.

4. Experimental Section

All DNA strands were purchased from Integrated DNA Technologies and purified using the PAGE purification method. A list of all DNA strands is shown in **Table 1**. Native PAGE and agarose gel were used to observe the thermodynamic equilibrium of localized DNA hybridization chain reactions. Ensemble fluorescence spectroscopy was used to monitor the real-time reaction kinetics of DNA hybridization reactions in the presence and absence of the DNA track. A reporter complex (RC), consisting of a Tetrachlorofluorescein fluorophore (TET) and an Iowa Black quencher molecule (FQ), was able to bind and give rise to fluorescence emission only when the stem and loop of hairpin H_6 were opened (Figure 1C). An equimolar solution of hairpins was mixed together. For the hairpin solution with the long DNA track, the solution was quickly heated at 90 °C for 10 min and was let to cool down to room temperature prior fluorescence kinetic experiments. The fluorophore was excited at 524 nm and the emission measured at 541 nm. The excitation and emission slits were set at 10 and 5 nm, respectively. For localized DNA hybridization reactions, 100 µL of 30×10^{-9} M sample was filled into a cleaned cuvette. All measurements were performed at 25 °C. For kinetic measurements, 1–10 µL of initiator strand was added

Table 1. DNA oligomers to assemble linear cascade DNA hybridization chain reactions on the long DNA track. Note: Toehold domains (colored green), stem domains (colored blue), clamp domains (colored red), spacer and linker domains (colored black), anchor domains (colored brown). In hairpin sequences, stems are underlined. For kinetic studies, the reporter complex (RC) is displaced by the highlighted domain of H_6.

Name	Sequence (5′ to 3′)	Length
Hairpin H_1	A1 5′ – GGGTGGGTTGTGATGTATGTAATGTTTTCCTCCTACTCACATACATCACAAC – 3′	52
Hairpin H_2	5′ – ACTCACATACATCAATCGTCTTTCTTTTGTTGTGATGTATGTGAGTAGGAGG – 3′ A2	52
Hairpin H_3	A3 5′ – GAAAGACGATTGATGTATGTGAGTTTTTCTTCCTTTAACATACATCAATCG – 3′	52
Hairpin H_4	5′ – TTTAACATACATCACCACTTTCCTTTTTCGATTGATGTATGTTAAAGGAAGA – 3′ A4	52
Hairpin H_5	A5 5′ – AGGAAAGTGGTGATGTATGTTAAATTTTCTTCTCCTCCACATACATCACCAC – 3′	52
Hairpin H_6	5′ – CTCCACATACATCATATTCCCTCATTCAAGCGTGGTGATGTATGTGGAGGAGAAG – 3′ A6	55
Initiator I	5′ – CATTACATACATCACAACCCACCC – 3′	24
RC FQ	5′ – TTGAATGAGGGAATATGATGTATGTGG/Quencher/ – 3′	27
RC TET	5′ – /Fluorophore/CCACATACATCATATTCCCT – 3′	20
Anchor A_1	5′ – TTGAGAGTAGTGGAGGAGAGGAGA – H1	24
Anchor A_2	H2 – AGAAGGAAGGAAAGGAAAGAAGGA – 3′	24
Anchor A_3	5′ – TTGGTGTGGTGTGGTGTGGTGGTG – H3	24
Anchor A_4	H4 – GGAGGAGGAGAAGGAGAGGAGAGA – 3′	24
Anchor A_5	5′ – GAAGTGAAGAAGAAGAAAGAGAAG – H5	24
Anchor A_6	H6 – GAAGAAAGAAGAAGAAGAGAGAAA – 3′	24
Track LT	5′ – TTTCTCTCTTCTTCTCTTCTTCTTCACTTCTCTCTCCTCTCCTTCACCACAC CACACCAATCCTTCTTTCCTTTCCTCCACTACTCTCAA – 3′	90

to a 100 µL sample. For nonlocalized DNA hybridization reactions, 80 µL of 5×10^{-9} M sample was used. Rapid mixing was achieved by carefully but quickly pipetting the whole volume up and down for a minute without generation of air bubbles or loss of material. All experiments were performed in 1× TAE Mg^{2+} buffer solution.

Supporting Information

Supporting Information is available from the Wiley Online Library or from the author.

Acknowledgements

This work was supported by NSF grants CCF-1217457, CCF-1141847, CCF-1617791, and CCF-1320360.

[1] B. Yurke, A. J. Turberfield, A. P. Mills, F. C. Simmel, J. L. Neumann, *Nature* **2000**, *406*, 605.
[2] G. Seelig, B. Yurke, E. Winfree, in *DNA Computing*, Vol. *3384* (Eds: C. Ferretti, G. Mauri, C. Zandron), Springer, Berlin **2005**, pp. 329–343.
[3] D. Y. Zhang, A. J. Turberfield, B. Yurke, E. Winfree, *Science* **2007**, *318*, 1121.
[4] G. Seelig, D. Soloveichik, D. Y. Zhang, E. Winfree, *Science* **2006**, *314*, 1585.
[5] D. Soloveichik, G. Seelig, E. Winfree, *Proc. Natl. Acad. Sci. USA.* **2010**, *107*, 5393.
[6] D. Y. Zhang, E. Winfree, *J. Am. Chem. Soc.* **2009**, *131*, 17303.
[7] L. Qian, E. Winfree, *Science* **2011**, *332*, 1196.
[8] L. Qian, E. Winfree, J. Bruck, *Nature* **2011**, *475*, 368.
[9] D. Y. Zhang, G. Seelig, *Nat. Chem.* **2011**, *3*, 103.
[10] D. Y. Zhang, S. X. Chen, P. Yin, *Nat. Chem.* **2012**, *4*, 208.
[11] D. Y. Zhang, *J. Am. Chem. Soc.* **2011**, *133*, 1077.
[12] A. J. Genot, D. Y. Zhang, J. Bath, A. J. Turberfield, *J. Am. Chem. Soc.* **2011**, *133*, 2177.
[13] D. Y. Zhang, E. Winfree, *Nucleic Acids Res.* **2010**, *38*, 4182.
[14] H. Chandran, N. Gopalkrishnan, A. Phillips, J. Reif, in *DNA Computing and Molecular Programming*, Vol. *6937* (Eds: L. Cardelli, W. Shih), Springer, Berlin **2011**, pp. 64–83.
[15] F. Dannenberg, M. Kwiatkowska, C. Thachuk, A. Turberfield, in *DNA Computing and Molecular Programming*, Vol. *8141* (Eds: D. Soloveichik, B. Yurke), Springer International Publishing, Temple, AZ **2013**, pp. 31–45.
[16] N. Dalchau, H. Chandran, N. Gopalkrishnan, A. Phillips, J. Reif, *ACS Synth. Biol.* **2015**, *4*, 898.
[17] R. A. Muscat, K. Strauss, L. Ceze, G. Seelig, in *ISCA'13: Proc. 40th Annual Int. Symp. Computer Architecture*, Vol. *41* (Ed: A. Mendelson), ACM, Tel-Aviv, Israel **2013**, pp. 177–188.
[18] E. Kopperger, T. Pirzer, F. C. Simmel, *Nano Lett.* **2015**, *15*, 2693.
[19] M. Teichmann, E. Kopperger, F. C. Simmel, *ACS Nano* **2014**, *8*, 8487.
[20] I. M. Ruiz, J. M. Arbona, A. Lad, O. Mendoza, J. P. Aime, J. Elezgaray, *Nanoscale* **2015**, *7*, 12970.
[21] R. M. Dirks, N. A. Pierce, *Proc. Natl. Acad. Sci. USA.* **2004**, *101*, 15275.

[22] S. Venkataraman, R. M. Dirks, P. W. K. Rothemund, E. Winfree, N. A. Pierce, *Nat. Nanotechnol.* **2007**, *2*, 490.
[23] D. Lubrich, S. J. Green, A. J. Turberfield, *J. Am. Chem. Soc.* **2009**, *131*, 2422.
[24] H. M. T. Choi, J. Y. Chang, L. A. Trinh, J. E. Padilla, S. E. Fraser, N. A. Pierce, *Nat. Biotechnol.* **2010**, *28*, 1208.
[25] W. J. Meng, R. A. Muscat, M. L. Mckee, P. J. Milnes, A. H. El-Sagheer, J. Bath, B. G. Davis, T. Brown, R. K. O'Reilly, A. J. Turberfield, *Nat. Chem.* **2016**, *8*, 542.
[26] P. Yin, H. M. T. Choi, C. R. Calvert, N. A. Pierce, *Nature* **2008**, *451*, 318.
[27] J. P. Sadowski, C. R. Calvert, D. Y. Zhang, N. A. Pierce, P. Yin, *ACS Nano* **2014**, *8*, 3251.
[28] S. Garg, *Ph.D. Thesis*, Duke University **2016**.
[29] P. W. K. Rothemund, *Nature* **2006**, *440*, 297.

Received: September 6, 2016
Revised: December 15, 2016
Published online:

